Journal of Magnetic Resonance 245 (2014) 50–57

Contents lists available at ScienceDirect

Journal of Magnetic Resonance

journal homepage: www.elsevier.com/locate/jmr

Optimal dielectric and cavity configurations for improving the efficiency of electron paramagnetic resonance probes

Sameh Y. Elnaggar [a], Richard Tervo [a], Saba M. Mattar [b,*]

[a] Department of Electrical and Computer Engineering, University of New Brunswick, Fredericton, New Brunswick, E3B 5A3 Canada
[b] Department of Chemistry and Centre for Laser, Atomic and Molecular Sciences, University of New Brunswick, Fredericton, New Brunswick E3B 5A3, Canada

ARTICLE INFO

Article history:
Received 21 March 2014
Revised 24 May 2014
Available online 6 June 2014

Keywords:
Electron paramagnetic resonance
Dielectric resonators
Resonant cavity
Resonator modes
Coupled mode theory
Coupled modes
Coupling coefficients
Quality factor
Filling factor
Finite element methods
Field distributions
Spectrometer sensitivity
Signal-to-noise ratio
Efficiency parameter

ABSTRACT

An electron paramagnetic resonance (EPR) spectrometer's lambda efficiency parameter (Λ) is one of the most important parameters that govern its sensitivity. It is studied for an EPR probe consisting of a dielectric resonator (DR) in a cavity (CV). Expressions for Λ are derived in terms of the probe's individual DR and CV components, Λ_1 and Λ_2 respectively. Two important cases are considered. In the first, a probe consisting of a CV is improved by incorporating a DR. The sensitivity enhancement depends on the relative rather than the absolute values of the individual components. This renders the analysis general. The optimal configuration occurs when the CV and DR modes are nearly degenerate. This configuration guarantees that the probe can be easily coupled to the microwave bridge while maintaining a large Λ. It is shown that for a lossy CV with a small quality factor Q_2, one chooses a DR that has the highest filling factor, η_1, regardless of its Λ_1 and Q_1. On the other hand, if the CV has a large Q_2, the optimum DR is the one which has the highest Λ_1. This is regardless of its η_1 and relative dielectric constant, ε_r. When the quality factors of both the CV and DR are comparable, the lambda efficiency is reduced by a factor of $\sqrt{2}$. Thus the signal intensity for an unsaturated sample is cut in half. The second case is the design of an optimum shield to house a DR. Besides preventing radiation leakage, it is shown that for a high loss DR, the shield can actually boost Λ above the DR value. This can also be very helpful for relatively low efficiency dielectrics as well as lossy samples, such as polar liquids.

1. Introduction

Continuous-wave (CW) and pulsed electron resonance techniques [1,2] such as electron paramagnetic resonance (EPR) [3], electron-electron double resonance (ELDOR) [4,5], double quantum coherence (DQC) [6–8], electron spin echo envelope modulation (ESEEM) [9,10] and electron-nuclear double resonance (ENDOR) [11,12] are powerful techniques for investigating the properties of unpaired electrons and paramagnetic molecules in physics, chemistry, structural biology, photosynthesis, surface science, catalysis [13], molecular magnetism and quantum computing [14].

The absolute spin sensitivity for very small samples, mostly due to their reactivity, is generally low. Consequently, a large amount of research is spent on increasing the sensitivity of such spectrometers. To increase the sensitivity miniature loop-gap (LGR) [15–17] or dielectric (DR) [18–25] resonators are used as probe components. Due to their small sizes, these resonators, have high energy density in the sample vicinity, large magnetic fields (B_1) and filling factors (η) [16–22,24–27].

To confine the microwave radiation, the probe normally has a shield that also houses its LGRs or DRs. Cavities (CVs) serve the same purpose as microwave shields and have also been used to house LGRs and DRs [28]. A single resonator placed in a TE_{102} cavity was used by different groups [18,19,24–27]. In our laboratory, a different tunable DR/TE_{102} probe was designed. It consists of two dielectric resonators, with $\varepsilon_r = 29.2$, that are asymmetrically placed in an unmodified TE_{102} rectangular cavity. Its signal to-noise-ratio (SNR) is at least 24 times larger than the TE_{102} cavity alone [21]. The frequency, field distributions and filling factors of the DR/TE_{102} probe were simulated and analyzed by finite element methods. From this study resonant cavity was determined to be an essential component of the probe and affects its frequency [29].

Because the size of the DR is much smaller than that of the CV, the filling factor of the probe increases. This is attributed to the concentration of the magnetic field inside the DR and in its vicinity [22]. When the two uncoupled modes of the DR and CV are degenerate, the interaction between their modes is a maximum [30]. This situation is very helpful in an experiment where the signal

* Corresponding author. Fax: +1 506 453 4981
E-mail address: mattar@unb.ca (S.M. Mattar).

http://dx.doi.org/10.1016/j.jmr.2014.05.011
1090-7807/

intensity of a standard conventional CV needs to be improved while leaving the coupling to the microwave bridge intact [22]. However if the signal enhancement is of higher priority to the spectroscopist, the DR should be housed in a small shield instead of a normal CV [18,31]. In the latter case, unless the shield is very tight, coupling to the microwave bridge through an iris may be difficult [31]. Inserting two stacked DRs in a CV gives the user the extra ability to tune the frequency of the probe [21,29,32].

Many reviews of the factors that affect the intensity of an EPR signal have been written. Some of these factors are specific to the spectrometer's probe while others depend on the properties of the paramagnetic sample [22,33,34]. The signal voltage, V_S, at the spectrometer's diode detector or mixer, is directly proportional to the signal intensity, I. The Intensity I is in turn obtained from V_S by a variety of methods. These may be magnetic field modulation and lock-in detection or direct detection using point digitizers, box car integrators or transient recorders. The voltage V_S takes the form [35–38].

$$V_S = \chi'' \eta Q \sqrt{PZ_0}, \tag{1}$$

where P is the incident microwave power coupled to the probe and Z_0 is the characteristic impedance of the microwave bridge. The χ'' term is the imaginary component of the sample's magnetic susceptibility. For simplicity and when the sample is unsaturated, the signal intensity, I, depends on the relevant spectrometer parameters as

$$I \propto \eta Q \sqrt{P}. \tag{2}$$

As pointed out earlier, although the presence of the DR leads to an increase in η, the decrease in Q may reduce the signal intensity [22,31]. For a small DR quality factor, Q_1, the signal enhancement, I_{probe}/I_{CV}, is found to be [38].

$$\frac{I_{probe}}{I_{CV}} \approx \frac{\eta_1}{\eta_2} \times \frac{Q_1}{Q_2}, \tag{3}$$

where I_{probe} is the intensity of the probe with an inserted DR and I_{CV} is the intensity of an empty cavity. The quality and filling factors of the DR and CV modes are denoted by Q_1, Q_2, η_1 and η_2 respectively. For example this situation occurs, in an experiment where the sample or solvent is a dipolar liquid leading to $Q_1 \ll Q_2$. In this case the losses of the sample can be lumped with those of the DR. On the other hand when $Q_1 \gg Q_2$, the signal enhancement is given by [38]

$$\frac{I_{probe}}{I_{CV}} \approx \frac{\eta_1}{\eta_2}. \tag{4}$$

In another words, for a large Q_1, the signal enhancement depends solely on the ratio of η_1 and η_2. The signal intensity I_{probe} was calculated at the frequency of the coupled modes while I_{CV} was calculated at the CV frequency ω_2.

Throughout the manuscript Λ, Q and η denote the overall probe's efficiency parameter, quality factor and filling factor, while Λ_1, Q_1 η_1, Λ_2, Q_2 η_2 are those of the dielectric resonator and cavity respectively.The Λ parameter is crucial in understanding the properties of EPR probes as it is a function of η and Q. In general, Λ, is defined as [31]

$$\Lambda = \frac{B_m}{2\sqrt{P}}, \tag{5}$$

where B_m is the magnetic field density at the sample. Here the sample is assumed to be small. For a small Q_1 the signal enhancement depends on the filling and quality factors. It is thus more convenient to express I_{probe}/I_{CV} in terms of Λ_1 and Λ_2 [31,34]. For unsaturated samples

$$\frac{I_{probe}}{I_{CV}} \approx \frac{\Lambda_1^2}{\Lambda_2^2}. \tag{6}$$

Using a lumped circuit model, the coupling between the $TE_{01\delta}$ DR mode and the TE_{011} CV mode was studied, where Λ and other parameters were calculated [31]. It was found that Λ is close to the intrinsic DR value. It was also shown that when the DR and CV are degenerate, Λ is approximately 98.5% of that of Λ_1.

The current authors formulated a coupled mode theory (CMT) to study the interaction between the DR and CV [30,38]. In fact, CMT was used to predict and calculate the frequencies and eigenvectors of the coupled modes [30]. Expressions for the coupling coefficient κ, Q and η of the coupled system were determined in terms of the corresponding uncoupled ones [38]. It was shown that η and Q are very sensitive to the frequency difference between the two uncoupled modes [31,38]. Therefore taking this into account, an EPR probe can be optimally designed.

The Λ parameter is the most convenient way to assess a probe's sensitivity. The aim of the current paper is to aid in the development of sensitive probes in terms Λ_1, Λ_2, η_1, η_2, Q_1 and Q_2. The derived expressions, that link these parameters, are then applied to study two important cases. The first one deals with the selection of an appropriate DR for a given CV. The second case is the design of an optimal shield or CV to house a given DR.

Section 2 describes the properties of the probe such as the frequencies, eigenvectors and the electric fields. In addition, expressions for the probe's κ, Q and η are presented. Finally, expressions for Λ are derived. Section 3 applies the results obtained for different situations. Two experimental conditions are discussed in detail. The results are verified using finite element simulations. Summary and conclusions are provided in Section 4.

1.1. Theoretical background

The fields of the coupled system are shown in Fig. 1. The system consists of a DR inserted in the center of a cylindrical CV. The holder is not taken into account because it is assumed to be of a low loss and low permittivity material. Therefore its effect is considered to be negligible.

The two uncoupled modes of interest are the $TE_{01\delta}$ mode of the DR and the TE_{011} mode of the CV. As shown in Fig. 1, the two uncoupled modes interact to form the coupled symmetric and anti-symmetric modes [30]. Coupling with other modes was previously discussed and it was shown that its effect is negligible [30,38].

This coupled system was previously considered [30]. The master equation which governs the system's behavior is in the form of an eigenvalue problem. It was solved and the parameters describing the coupled system were determined. The coupling coefficient (κ) is,

$$\kappa = \frac{\varepsilon_0(\varepsilon_r - 1)\int_{DR} \vec{E}_1^{*} \cdot \vec{E}_2 dv}{\sqrt{H_{11}H_{22}}}. \tag{7}$$

The eigenvalues (ω^{++}, ω^{+-}) and the eigenvectors (a_i^{++}, a_i^{+-}) were found to be [30]

$$\omega^{2++} = \frac{\omega_1^2 + \omega_2^2}{2} - \sqrt{\left(\frac{\omega_1^2 - \omega_2^2}{2}\right)^2 + \omega_1^2\omega_2^2\kappa^2}, \tag{8}$$

$$a_2^{++} = \left(\frac{1}{2\kappa}(\gamma^2 - 1) + \sqrt{\frac{1}{4\kappa^2}(\gamma^2 - 1)^2 + \gamma^2}\right) a_1^{++} \tag{9}$$

for the symmetric mode and

$$\omega^{2+-} = \frac{\omega_1^2 + \omega_2^2}{2} + \sqrt{\left(\frac{\omega_1^2 - \omega_2^2}{2}\right)^2 + \omega_1^2\omega_2^2\kappa^2} \tag{10}$$

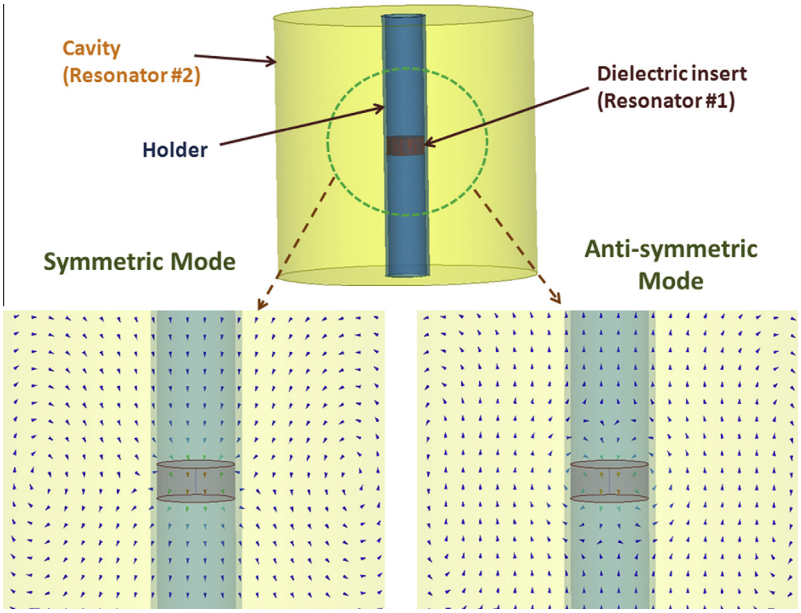

Fig. 1. Schematic diagrams of the symmetric and anti-symmetric modes of a DR inserted in a conducting CV. The DR is held inside a hollow low loss and low permittivity holder.

$$a_2^{+-} = \left(\frac{1}{2\kappa}(\gamma^2-1) - \sqrt{\frac{1}{4\kappa^2}(\gamma^2-1)^2+\gamma^2}\right)a_1^{+-} \tag{11}$$

for the anti-symmetric mode. Here γ^2 is equal to

$$\gamma^2 = \left(\frac{\omega_1}{\omega_2}\right)^2. \tag{12}$$

The quality factor, is a function of the uncoupled Q_1 and Q_2. A closed form expression for Q is [38]

$$Q = \frac{\omega}{\frac{|a_1|^2\omega_1}{Q_1}+\frac{|b_2|^2\omega_2}{Q_2}} \tag{13}$$

and the power loss for the probe is found to be

$$P_l = |a_1|^2 P_l^{(1)} + |a_2|^2 P_l^{(2)} \tag{14}$$

$$P_l = \frac{1}{2}\left(\frac{\omega_1|a_1|^2}{Q_1}+\frac{\omega_2|a_2|^2}{Q_2}\right), \tag{15}$$

where $P_l^{(1)}$ and $P_l^{(2)}$ are the DR and CV power losses respectively. The DR losses, $P_l^{(1)}$, are due to the dielectric losses (loss tangent). The radiation losses vanish once the DR in enclosed in the CV. The power loss due to the microwave bridge iris can be included by noting that it occurs at the iris-CV interface and is mainly due to the CV fields. Thus Q_2 is taken to be the quality factor of the loaded CV [38]. Similarly, the η of the coupled system is [38]

$$\eta = |a_1|^2\eta_1 + |a_2|^2\eta_2. \tag{16}$$

1.2. Derivation of the probe lambda efficiency

To calculate the lambda efficiency, B_1 and P_l are needed. Obviously these two parameters depended on the coupling method. The P_l is affected by the iris and this is taken into account using the loaded Q. The magnetic field, can be determined from the electric field using Maxwell's equation

$$\mathbf{B} = -\frac{1}{j\omega}\nabla\times\mathbf{E}, \tag{17}$$

where ω is the mode resonant frequency. Here it is assumed that B_1 fully excites the appropriate mode.

Equipped with Eqs. (5), (14), and (15) presented in the previous sections, one finds expressions for Λ. The magnetic field $\vec{B}$ is expanded in terms of the uncoupled fields as [30]

$$\vec{B} = b_1\vec{B}_1 + b_2\vec{B}_2, \tag{18}$$

where b_1 and b_2 are the expansion coefficients. The probe Λ is then

$$\Lambda = \frac{|b_1B_{1m}+b_2B_{2m}|}{2\sqrt{P_l}}. \tag{19}$$

Here P_l is given by Eq. (15). In the steady state, it is equal to the power coupled to the probe [15].

The variables B_{1m} and B_{2m} are the maximum magnetic field densities of the DR and CV respectively. The sample is small and is located at the maximum magnetic field density. Since κ is small then $b_i \approx a_i$ [30]. After some algebraic manipulation, Λ can be related to the uncoupled ones as

$$\Lambda = \frac{1}{\sqrt{1+\xi^2}}|\Lambda_1 + \xi\Lambda_2|, \tag{20}$$

where

$$\Lambda_1 = \frac{B_{1m}}{2\sqrt{P_{l1}}} \tag{21}$$

and

$$\Lambda_2 = \frac{B_{2m}}{2\sqrt{P_{l2}}}. \tag{22}$$

They are the DR and CV lambda efficiencies respectively while ξ is equal to

$$\xi = \frac{a_2}{a_1}\sqrt{\left(\frac{Q_1}{Q_2}\times\frac{\omega_2}{\omega_1}\right)}. \tag{23}$$

When the two resonators are degenerate, $a_1 = \pm a_2$ and $P_l = (P_{l1} + P_{l2})/2$. Therefore Eq. (19) reduces to

$$\Lambda = \left|\frac{B_{1m}}{2\sqrt{P_{l1}+P_{l2}}} \pm \frac{B_{2m}}{2\sqrt{P_{l1}+P_{l2}}}\right|. \tag{24}$$

Eq. (24) simply indicates that, when the DR and CV are degenerate, and the total losses taken into account, Λ of the symmetric mode is the sum of the modified Λ_1 and Λ_2. Similarly, Λ of the anti-symmetric mode is the difference of Λ_1 and Λ_2.

2. Results and discussion

In this section the formulae derived in the previous section will be applied to different cases. Because of their importance, expressions (19) and (20) are calculated for a typical probe that was previously studied [30,31,38]. In this case, the DR has an $\varepsilon_r = 261$ and $f_{TE_{01\delta}} = 9.5$ *GHz*. The aspect ratio of the diameter to height is unity and the dielectric loss tangent is 7.5×10^{-4} ($Q_1 = 1333.33$). The DR diameter and height are allowed to change from 1.3 to 2.1 mm. The CV is silver plated resulting in $Q_2 \approx 32,000$. Both the CV diameter and height are equal to 4.1598 cm. These dimensions guarantee that its resonant frequency $f_{TE_{011}} = 9.5$ *GHz*. The calculated Λ versus the DR diameter is depicted in Fig. 2.

The Λ values calculated using CMT shown in Fig. 2 are in excellent agreement with those obtained previously [31]. Therefore, Eqs. (19) and (20), derived in the previous section, can be used to study the behavior of Λ for different configurations.

Normally, experimentalists are interested in enhancing the SNR of their spectrometers. This implies the improvement of its probe Λ factor. In the next two subsections, two important cases are discussed. In the first case, a suitable DR is needed to enhance the signal intensity of a given CV. Here the parameters of the enclosing CV are fixed. In the second case, a housing shield (or a CV) is required which maximizes Λ of the whole probe.

2.1. Improving the probe's Λ by incorporating a DR

The purpose of adding a DR to a CV is to improve the overall probe's Λ without changing the coupling mechanism to the microwave bridge. Usually the microwave modes are excited through an iris on the CV wall. To excite these modes, the fields of the probe should have a significant value in the vicinity of the CV wall. Thus it is preferable to work near degeneracy ($\omega_1 \approx \omega_2$) where the coupled fields contain approximately equal contributions from both the DR and CV fields. Because the CV component is significant, coupling to the microwave bridge through the cavity iris can be easily achieved. Accordingly in this paper, the behavior of the probe when the DR and CV are nearly degenerate is examined. For the sake of completeness, the two limiting cases when $\omega_1 \gg \omega_2$ and $\omega_2 \gg \omega_1$ are given in the Appendix. In this subsection it is assumed that the CV has fixed lambda efficiency Λ_2.

When the DR and CV frequencies are nearly degenerate, $\omega_1 - \omega_2$ is relatively small and the ratio a_2/a_1 is found, from Eqs (9) and (11), to be

$$\frac{a_2}{a_1} \approx \pm 1. \tag{25}$$

Here the plus sign corresponds to the symmetric mode while the minus sign to the anti-symmetric mode.

The main aim in this subsection is to improve the efficiency of the probe with respect to that of the CV. Thus one needs to maximize Λ/Λ_2. From Eq. (20)

$$\frac{\Lambda}{\Lambda_2} = \frac{1}{\sqrt{1+\xi^2}}\frac{\Lambda_1}{\Lambda_2} + \xi. \tag{26}$$

Substituting Eqs. (23) and (25) in (26) gives

$$\frac{\Lambda}{\Lambda_2} = \frac{1}{\sqrt{1+\left(\frac{Q_1}{Q_2}\right)\left(\frac{\omega_2}{\omega_1}\right)}}\left(\frac{\Lambda_1}{\Lambda_2}\right) \pm \sqrt{\left(\frac{Q_1}{Q_2}\right)\left(\frac{\omega_2}{\omega_1}\right)}. \tag{27}$$

Thus Λ/Λ_2 is a function of Λ_1/Λ_2, Q_1/Q_2 and ω_2/ω_1. This dependency on ratios renders the analysis simpler and scalable. To investigate the behavior of Λ/Λ_2 as a function of Λ_1/Λ_2 and ω_2/ω_1, one assumes a set of hypothetical DRs that have the same Λ_1. It can be achieved, at least in theory, by changing η_1 accordingly and covers all possible situations. This assumption is purely mathematical and does not influence the final physical conclusions. Consequently Λ/Λ_2 can be represented as a family of surfaces. Each surface represents a constant Λ_1/Λ_2. For the sake of clarity two such surfaces are plotted in Fig. 3a and b. The surface in Fig. 3a is for $\Lambda_1/$

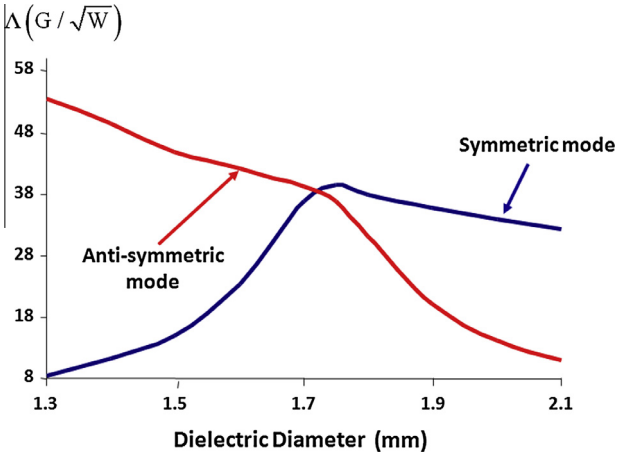

Fig. 2. The Λ factor for both the symmetric and the anti-symmetric modes of a probe consisting of a DR ($\varepsilon_r = 261$) inserted in a silver plated cylindrical CV. For easy comparison with Ref. [31] Λ is plotted versus the DR diameter.

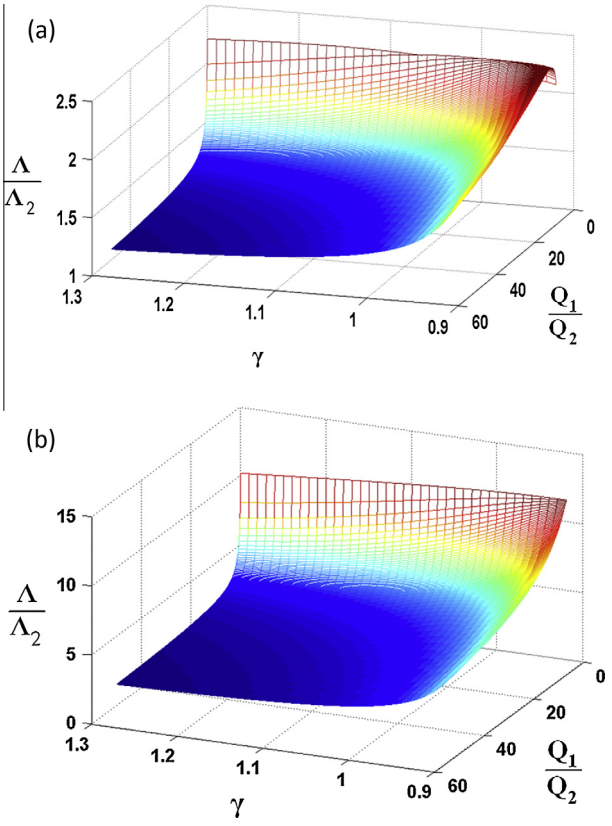

Fig. 3. The normalized Λ as a function of the relative frequency and the relative quality factor. In Fig 3a $\Lambda_1/\Lambda_2 = 2$, $\kappa = 0.125$ and $\varepsilon_r = 20.0$ while in Fig 3b $\Lambda_1/\Lambda_2 = 11.5$, $\kappa = 0.15$ and $\varepsilon_r = 29.2$. Here $\gamma = \omega_1/\omega_2$.

$\Lambda_2 = 11.5$ where it encompasses typical probes that are commonly used [20,21,25,39,40]. In particular, Λ_2 for a typical silver plated cylindrical cavity is $\approx 2G/\sqrt{W}$ and $\Lambda_1 \approx 23G/\sqrt{W}$ (Murata DRD06 00265R®). Fig 3b represents $\Lambda_1/\Lambda_2 = 2$ surface. This occurs for a lossy sample inserted in a DR where the effective Λ_1 is low ($\Lambda_1 = 4G/\sqrt{W}$and $\tan(\delta_{sample}) \approx 2 \times 10^{-3}$).

The behavior of Λ/Λ_2 in Fig. 3a and b is very similar and strongly depends on Q_1/Q_2. Consequently three cases are carefully examined. The first is when $Q_1 \gg Q_2$. This occurs when a CV is overcoupled as in pulsed experiments or the CV is not silver plated. The second case is when $Q_1 \ll Q_2$. This is a common situation when using liquid polar samples inside the DR. In this case the sample losses decrease Q_1. The third case is the common one where $Q_1 \approx Q_2$.

From Fig. 3a and b, one can conclude that given a specific CV, a DR with a large Λ_1 and a relatively low Q_1, Λ is comparable to that of Λ_1. This is exactly the case examined in Ref. [31] ($\Lambda_1 \approx 40\ G/\sqrt{W}$, $Q_1 \approx 1333$, $\Lambda_2 \approx 2.5\ G/\sqrt{W}$, $Q_2 \approx 32,000$) where $\Lambda_1/\Lambda_2 = 16$. Fig. 4 illustrates how this surface behaves when the DR and CV frequencies are nearly degenerate ($\gamma \approx 1$).

As seen from this figure when $Q_1 \ll Q_2$, which is the condition used in Ref. [31], Λ is approximately equal to that of the DR, Λ_1. From a spectroscopist's perspective, this means that the DR with a high Λ_1 and not necessarily the highest ε_r gives the best signal enhancement.

Fig. 4 also shows that for the second case where, $Q_1 \gg Q_2$, Λ is small. In this case, its value can be estimated by knowing that $\xi = \sqrt{Q_1/Q_2}$, and Eq. (20) reduces to

$$\Lambda \approx \frac{\Lambda_1}{\xi} + \Lambda_2. \tag{28}$$

Because Q_2 is small, Λ_2 is small enough to be ignored. Thus Λ is written as

$$\Lambda \approx \frac{\Lambda_1}{\xi} \approx \frac{B_{1m}}{2\sqrt{P_{l2}}}. \tag{29}$$

Eq. (29) indicates that Λ can be controlled by the DR's magnetic field, B_{1m} and is limited by the CV losses. The smaller the DR the higher is its B_{1m}. The maximum B_{1m} value depends on the dielectric constant, the DR's dimensions and filling factor, η_1. Thus regardless of the exact DR's Q_1 value (as long as $Q_1 \gg Q_2$) the signal enhancement, which depends on Λ, is a function of the η_1 alone. Therefore one may conclude that, for low quality cavities the main parameter affecting the signal enhancement is the DR filling factor, η_1, while the DR's quality factor, Q_1 and Λ_1, have an insignificant contribution.

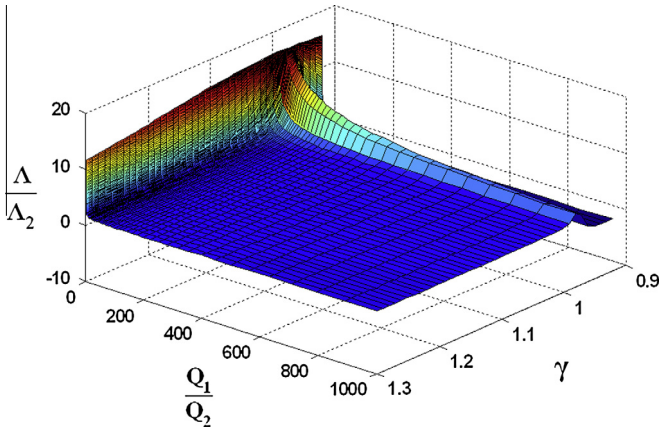

Fig. 4. The normalized Λ as a function of the relative frequency and the relative quality factor for a probe consisting of a cavity and a ferroelectric DR. Here $\Lambda_1/\Lambda_2 = 16$.

To better clarify the above scenarios, the HFSS eigenmodes solver is used to calculate Λ for typical probe components. The results are given in Table 1. The HFSS program (Ansys Corporation, Pittsburgh, PA, USA) uses finite element methods to numerically solve for the electromagnetic fields and frequencies subjected to the boundary conditions. The relative frequency tolerance was taken to be less than 0.1%.

From this table, for a low loss cavity ($Q_1 \ll Q_2$) the DR which has the highest Λ_1, in column 3, gives a better lambda efficiency of $20.96\ G/\sqrt{W}$ compared to $12.44G/\sqrt{W}$ in column 2. This is true although ε_r in column 3, and consequently η_1, have lower values. On the other hand for cavities with low Q_2 the DR used in column 4 that has the higher $\varepsilon_r = 29.2$ (higher η_1) leads to higher Λ (9.76) although it has the lower Λ_1 value (23.0) compared to the one in column 5.

Equations (3) and (4) are general and were derived previously in Ref. [38]. The conclusions obtained from Table 1 are in accordance with these two equations and are independent of the sample shape and size. Finally when the Qs of the two uncoupled resonators are close in value then $\xi \approx 1$ and Eq. (20) becomes

$$\Lambda = \frac{1}{\sqrt{2}}(\Lambda_1 + \Lambda_2). \tag{30}$$

To numerically verify this equation, the HFSS eigenmodes solver was used to calculate Λ of a Murata DRD0600265R® resonators ($\Lambda_1 = 23G/\sqrt{W}$) inserted in a 4.1598 cm × 4.1598 cm cylindrical cavity with $Q_2 = 15,000$. These dimensions guarantee that frequencies of both the DR and CV are degenerate. Calculations of Eq. (30) using Maple 13™ (MapleSoft, a subsidiary of Cybernet Systems Co. Ltd.) show that Λ is found to be $\approx 18G/\sqrt{W}$ which is very close to the HFSS result ($18.6G/\sqrt{W}$). Since usually $\Lambda_1 \gg \Lambda_2$, therefore Λ given by Eq. (30) can be simplified to

$$\Lambda \approx \frac{1}{\sqrt{2}}\Lambda_1. \tag{31}$$

From Eq. (31) it can be inferred that when the DR and CV modes are degenerate and their Qs are close in value, the signal enhancement for an unsaturated sample is half that of the DR alone.To summarize, the above discussions indicate Λ depends on the relative values of Q_1 and Q_2. When $Q_1 \ll Q_2$, its value approaches the DR intrinsic value. When $Q_1 \gg Q_2$, Λ is controlled by η_1 of the DR and limited by the CV losses. Finally when $Q_1 \approx Q_2$, Λ is approximately $1/\sqrt{2}$ times the DR intrinsic value. In this latter case, the signal intensity of the unsaturated sample is half that expected from the DR alone.

2.2. Choosing a shield for a given dielectric resonator

Given a DR with a certain Λ_1 and Q_1, one needs to choose a suitable CV that acts as an enclosing shield. The main requirement here is to maximize Λ.

Table 1
Lambda efficiency[a] for the cases $Q_1 \ll Q_2$, and $Q_1 \gg Q_2$.

Relative Q	$Q_1 \ll Q_2$		$Q_1 \gg Q_2$	
ε_r	261	29.2	29.2[b]	24[c]
Q_1	133	15,000	15,000	35,000
Q_2	30,000	30,000	3000	3000
Λ_1	12.65	23	23	32.34
Λ_2	2.5	2.5	0.776	0.776
Λ	12.44	20.96	9.76	7.64

[a] Λ Units in $G/\sqrt{W}$.
[b] Murata DRD0600265R® dielectric resonator.
[c] Murata DRD0650288F® dielectric resonator.

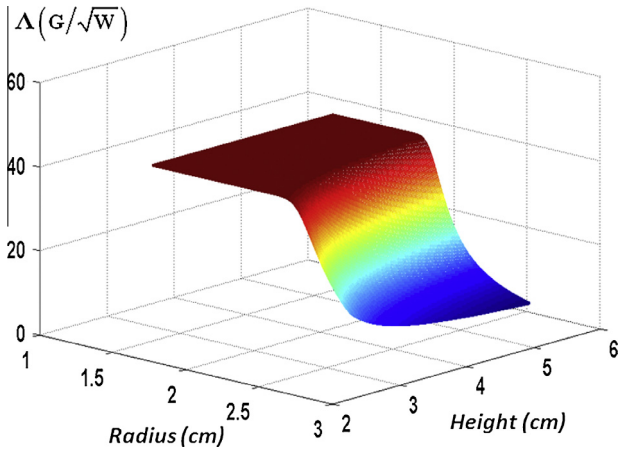

Fig. 5. Lambda efficiency of a probe as a function of the CV height and radius covering a wide range of frequencies. The DR has $\varepsilon_r = 261$, $\Lambda_1 = 40.0G/\sqrt{W}$, height = diameter = 1.75 mm (frequency = 9.5 GHz) of and $Q_1 = 1333.33$ enclosed in a silver plated shield.

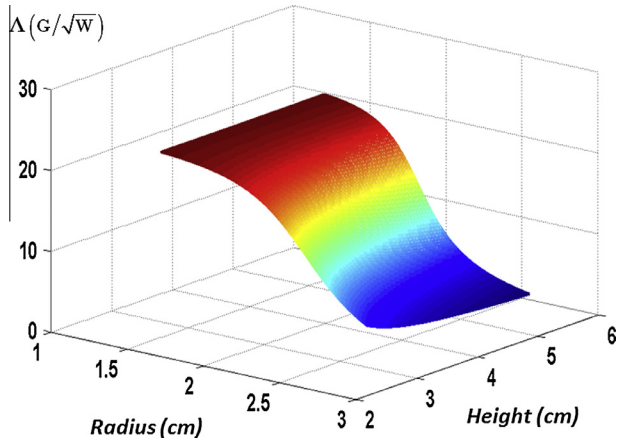

Fig. 6. Lambda efficiency of a probe as a function of the CV height and radius covering a wide range of frequencies. The DR has $\varepsilon_r = 29.2$, $\Lambda_1 = 23.0G/\sqrt{W}$, height = 2.65, diameter = 6.0 mm (frequency = 9.7 GHz) of and $Q_1 = 15{,}000$ enclosed in a copper shield with $\sigma = 5.8 \times 10^7$ S/m.

The behavior of Λ, determined by Eq. (20), is solved for different enclosing shield dimensions and the results are reported in Figs. 5 and 6 for typical DRs.

In general, Q_2, Λ_2 and TE_{011} frequency change with the CV dimensions. Therefore the formulae reported in the literature [31,41] were used to obtain Figs. 5 and 6.

Using the previously reported results for high permittivity DRs [31] and Figs. 5 and 6 it is seen that, when the shield gets smaller, Λ asymptotically approaches the dielectric value.

For DRs with low ε_r and low Q_1 or for high loss samples such as polar liquids, optimizing Λ is very important. Such DRs have moderately low Λ_1 so any boost from the shield is highly desirable. This accomplished by making use of Eq. (24). If the DR and CV are degenerate and $P_{l1} \gg P_{l2}$, Λ of the symmetric mode can be written as

$$\Lambda \approx \Lambda_1 + \frac{B_{2m}}{2\sqrt{P_{l1}}} - \frac{1}{2}\frac{P_{l2}}{P_{l1}}\left(\Lambda_1 + \frac{B_{2m}}{2\sqrt{P_{l1}}}\right). \tag{32}$$

When the net value of the second and third term at the right hand side of Eq. (32) is positive, then $\Lambda > \Lambda_1$. Starting from Eqs (21), (22) and using simple algebra, the condition at which $\Lambda > \Lambda_1$ is

$$\frac{B_{2m}}{B_{1m}} > \frac{1}{2}\frac{v}{1-v}, \tag{33}$$

where $v = P_{l2}/P_{l1} = Q_1/Q_2$. Therefore Eq. (33) can be approximated to

$$\frac{B_{2m}}{B_{1m}} > \frac{1}{2}\frac{Q_1}{Q_2}. \tag{34}$$

Compared to the DR, the fields in the cavity (or shield) are spread over a larger area and, in turn, $B_{2m} < B_{1m}$. Consequently when v is small, the condition (34) may be met particularly if the shield is designed as a long tube and the DR has a low Q value. To numerically show that the CV can indeed boost Λ according to Eq. (32) and (34), a structure composed of a long tube shield housing a DR with $\varepsilon_r = 20$, is simulated using CMT and verified by the HFSS eigenmodes solver. The lambda efficiency of the coupled system is calculated for different Q_2 values. The system structure and Λ are shown in Fig. 7.

As shown in Fig. 7, when the CV Q_2 is >8000 Λ is boosted (12.5% more than Λ_1). The shield was chosen such that the TE_{011} mode has the same frequency of the dielectric $TE_{01\delta}$ mode (11.3 GHz) i.e. the DR and CV are degenerate.

So far the inequality (34) assumed that the shield and the DR are degenerate. This is not usually the case. To relax this condition and to study the behavior of Λ, CMT is applied to different shield dimensions. The same DR, utilized in Fig. 7, is used. The results are presented in Fig. 8.

Fig. 8 shows that certain shield dimensions maximized Λ. One can pick a point on the surface maximum and calculate the value of Λ. One such point is when the shield's height is 6.0 cm and its radius is 1.95 cm. In this configuration the shield TE_{011} frequency is 9.7 GHz, which is lower than that of the DR (11.3 GHz). This means that the shield is large. Using Eq. (20)the value of Λ is found to be $4.57G/\sqrt{W}$. Applying the more accurate expression of Eq. (19), one finds that at $f^{++} \approx 9.58$ GHz Λ is equal to $5.47G/\sqrt{W}$. The corresponding value calculated using HFSS is $5.35G/\sqrt{W}$. This is very close to the value predicted by CMT. Thus by careful design, an enhancement in Λ can be achieved. In fact in this case, Λ has been improved by 35% resulting in 80% in signal intensity enhancement compared to Λ_1. Thus a large shield can boost Λ. The eigenvector is calculated using CMT and verifies that the mode is CV-like. Indeed if the uncoupled fields are normalized, one can find that $a_2/a_1 \approx 3.7$. Thus, it can be concluded that the mode is easily excited through an iris. It is worth noting that the optimum Λ

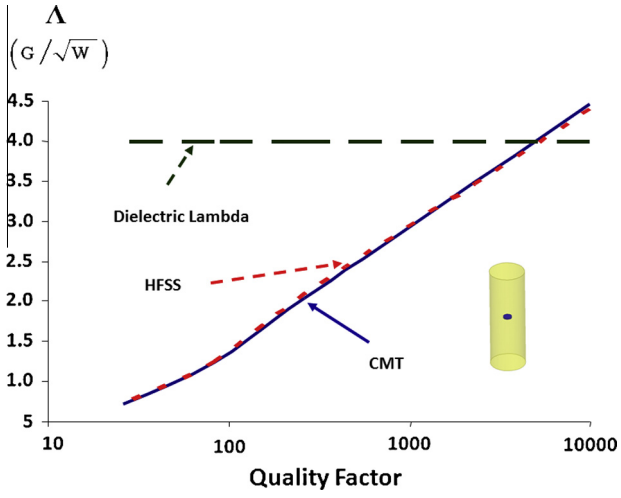

Fig. 7. The lambda efficiency of a dielectric inserted in a long shield versus the CV quality factor. The DR has $\varepsilon_r = 20.0$, $\Lambda_1 = 4.0G/\sqrt{W}$, height = 1.5, diameter = 4.0 mm and $Q_1 = 1000$. The CV height = 1.655 and diameter = 3.3 mm.

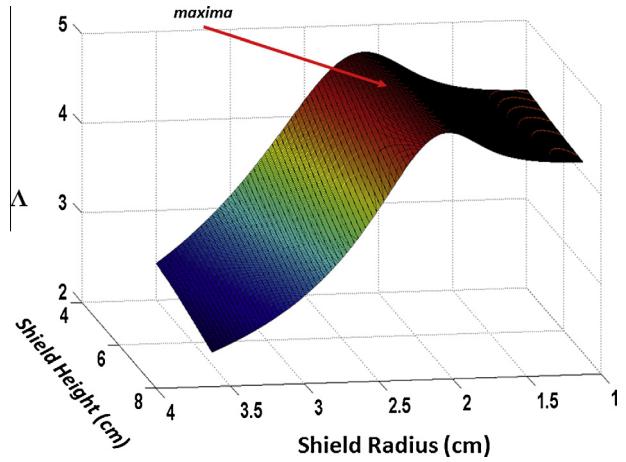

Fig. 8. Lambda efficiency for a coupled system consisting of a lossy dielectric resonator and a shield as a function of the shield dimensions. The DR has $\varepsilon_r = 20.0$, $\Lambda_1 = 4.0G/\sqrt{W}$, height = 1.5, diameter = 4.0 mm and $Q_1 = 1000$. The shield is silver plated and its conductivity $\sigma = 6.3 \times 10^7$ S/m.

occurs at a significantly lower frequency (9.38 GHz) compared to that of the DR (11.3).

Since CMT does not include the effect of the shield walls, HFSS was used to calculate Λ when the DR was enclosed in a small shield (Diameter = 2.8 cm, Height = 3.5 cm and $f_{TE_{011}} \approx 13.9$ GHz). The Λ value is found to be $\approx 6.3\,G/\sqrt{W}$ at $f^{++} \approx 11$ GHz. This means that the shield boosted Λ by 58% which translates into a 150% signal enhancement. This is because, for unsaturated samples, the signal ratio is proportional to Λ^2.

To better understand why the housing shield can improve Λ, we make reference to Eq. (24). For the symmetric mode, the equation shows that the fields of the CV and DR modes are in phase. This means that the B_{1m} and B_{2m} components reinforce one another. Thus according to Eqs (33), (34), Λ is boosted.

3. Summary and conclusions

Expressions for the lambda efficiency (Λ) of a system composed of a cavity with a dielectric insert in terms of those of the uncoupled ones (Λ_1 and Λ_2) were obtained. Two important situations are studied. The first is concerned with the selection of an appropriate DR for a given CV. While the second deals with the design of an optimal shield for a given DR. In the first situation it was shown that operating near the degenerate condition, where the fields are a mix of both the CV and DR fields, is the optimal configuration. In this situation, the coupling to the microwave bridge can be easily achieved through the CV iris. If the DR has a relatively high quality factor ($Q_1 \gg Q_2$), its filling factor, η_1, plays a dominant role in the signal enhancement, while the exact value of Q_1 and Λ_1 is irrelevant. Therefore for cavities with a small Q_2, the DR which has the highest η_1 results in the highest Λ efficiency. On the other hand, provided that $Q_1 \ll Q_2$, one should choose the resonator which has the highest Λ_1 regardless of the value of the filling factor, η_1.

It was also shown that when the two uncoupled systems (DR and CV) have the same quality factor, the signal enhancement for unsaturated samples is half that of the DR alone.

When choosing a shield for a particular DR, it was found that, in general, Λ asymptotically approaches the DR value when the shield gets tighter. However by careful design the shield can boost Λ of the probe for lossy DRs. This can be very helpful for relatively low efficiency DRs and for lossy samples such as polar liquids. Using both CMT and HFSS, it was shown that a tight shield can indeed boost the efficiency by 58%. Even for a large shield a boost in efficiency was predicted by CMT and verified by the HFSS eigenmodes solver. For the latter case, it was shown that the mode is predominantly CV in character. Accordingly, one may conclude that this mode can be easily coupled to the microwave bridge through an iris.

The current paper illustrates that the shield can improve Λ. From the expressions found here for Λ, it can be argued that a system consisting of different open structures (loop-gap, dielectric and split-ring resonators) may be used in a way such that their $\underline{B}_1$ values reinforce each other and hence increase Λ of the combined structure.

Acknowledgments

SMM acknowledges the Natural Sciences and Engineering Research Council of Canada for financial support in the form of a discovery (operating) grant. SYN is grateful for the financial assistance from the University of New Brunswick in the form of predoctoral teaching and research assistantships. We would also like to acknowledge CMC microsystems for providing the HFSS suite of programs that facilitated this research.

Appendix A

This Appendix deals with two limiting cases when trying to improve Λ of a probe by incorporating a DR.. To increase Λ one may be tempted to select a very small DR. In this case $\omega_1 \gg \omega_2$, and the CV is considered as a large shield. Consequently $a_2^{++}/a_1^{++} \to \infty$ and $a_2^{+-}/a_1^{+-} \to 0$. Therefore for the two coupled modes, Eq. (20) approaches

$$\Lambda^{++} = \Lambda_2 \tag{35}$$

for the symmetric mode, and

$$\Lambda^{+-} = \Lambda_1 \tag{36}$$

for the anti-symmetric mode.

Equation (36) reveals that, provided that a very small DR is used, the anti-symmetric mode has a large Λ efficiency. However due to the small field values near the cavity wall, it is difficult to excite this mode through the cavity iris [31]. Moreover, the DR mode may couple with higher CV modes. Therefore, this configuration is impractical [30].

The other extreme situation arises when the DR is large and $\omega_1 \ll \omega_2$. In this case, the CV acts as a small shield. Therefore $a_2^{++}/a_1^{++} \to 0$ and $a_2^{+-}/a_1^{+-} \to \infty$. Accordingly,

$$\Lambda^{++} \to \Lambda_1 \tag{37}$$

and

$$\Lambda^{+-} \to \Lambda_2. \tag{38}$$

Eq. (37) shows that Λ of the symmetric mode tends to that of the DR mode. This is because the fields of the symmetric mode tend to the DR uncoupled fields [30]. Depending on the DR size, this mode may be easily coupled to the microwave bridge. However because the CV dimension is fixed, the DR cannot be made very small. Moreover the larger the DR the lower its resonance frequency. This puts an upper limit on the DR Λ_1.

References

[1] C.P. Poole, Electron Spin Resonance, A Comprehensive Treatise on Experimental Techniques, second ed., John Wiley and Sons, New York, 1983.
[2] A. Schweiger, G. Jeschke, Principles of Pulsed Electron Paramagnetic Resonance, Oxford University Press, Oxford, 2001.

[3] M. Bennati, T.F. Prisner, New developments in high field electron paramagnetic resonance with applications in structural biology, Rep. Prog. Phys. 68 (2005) 411–448.
[4] L.D. Kispert, Electron-electron double resonance, Biol. Magn. Reson. 24 (2005) 165–197.
[5] Y.D. Tsvetkov, Peptide aggregation and conformation properties as studied by pulsed electron-electron double resonance: pulsed ELDOR in spin labeled peptides, Biol. Magn. Reson. 21 (2004) 385–433.
[6] P.P. Borbat, J.H. Davis, S.E. Butcher, J.H. Freed, Measurement of large distances in biomolecules using double-quantum filtered refocused electron spin-echoes, J. Am. Chem. Soc. 126 (2004) 7746–7747.
[7] Y.W. Chiang, P.P. Borbat, J.H. Freed, The determination of pair distance distributions by pulsed ESR using Tikhonov regularization, J. Magn. Reson. 172 (2005) 279–295.
[8] S.K. Misra, P.P. Borbat, J.H. Freed, Calculation of double-quantum-coherence two-dimensional spectra: distance measurements and orientational correlations, Appl. Magn. Reson. 36 (2009) 237–258.
[9] S.S. Eaton, G.R. Eaton, Measurements of interspin distances by EPR, Electron Paramagnetic Reson. 19 (2004) 318–337.
[10] J. McCracken, Electron spin echo envelope modulation (ESEEM) spectroscopy, Appl. Phys. Methods Inorg. Bioinorg. Chem. (2007) 55–77.
[11] G.R. Eaton, S.S. Eaton, Electron-nuclear double resonance spectroscopy and electron spin echo envelope modulation spectroscopy, Compr. Coord. Chem. II (2) (2004) 49–55.
[12] M.M. Hertel, V.P. Denysenkov, M. Bennati, T.F. Prisner, Pulsed 180-GHz EPR/ENDOR/PELDOR spectroscopy, Magn. Reson. Chem. 43 (2005) S248–S255.
[13] D. Goldfarb, Electron paramagnetic resonance applications to catalytic and porous materials, Electron Paramagnetic Reson. (2009) 451–487.
[14] S.S. Eaton, G.R. Eaton, The world as viewed by and with unpaired electrons, J. Magn. Reson. 233 (2012) 12.
[15] R.W. Dykstra, G.D. Markham, A dielectric sample resonator design for enhanced sensitivity of EPR spectroscopy, J. Magn. Reson. 69 (1986) 350–355.
[16] W. Froncisz, J.S. Hyde, The loop-gap resonator: a new microwave lumped circuit ESR sample structure, J. Magn. Reson. 47 (1982) 515–521.
[17] J.P. Hornak, J.H. Freed, Electron spin echoes with a loop-gap resonator, J. Magn. Reson. 62 (1985) 311–313.
[18] A. Blank, E. Stavitski, H. Levanon, F. Gubaydullin, Transparent miniature dielectric resonator for electron paramagnetic resonance experiments, Rev. Sci. Instrum. 74 (2003) 2853–2859.
[19] I. Golovina, I. Geifman, A. Belous, New ceramic EPR resonators with high dielectric permittivity, J. Magn. Reson. 195 (2008) 52–59.
[20] M. Jaworski, A. Sienkiewicz, C.P. Scholes, Double-stacked dielectric resonator for sensitive EPR measurements, J. Magn. Reson. (1969–1992) 124 (1997) 87–96.
[21] S.M. Mattar, A.H. Emwas, A tuneable doubly stacked dielectric resonator housed in an intact TE102 cavity for electron paramagnetic resonance spectroscopy, Chem. Phys. Lett. 368 (2003) 724–731.
[22] Y.E. Nesmelov, J.T. Surek, D.D. Thomas, Enhanced EPR sensitivity from a ferroelectric cavity insert, J. Magn. Reson. 153 (2001) 7–14.
[23] A. Raitsimring, A. Astashkin, J.H. Enemark, A. Blank, Y. Twig, Y. Song, T.J. Meade, Dielectric resonator for -band pulsed EPR measurements at cryogenic temperatures: probehead construction and applications, Appl. Magn. Reson. 42 (2012) 441–452.
[24] F.J. Rosenbaum, Dielectric cavity resonator for ESR experiments, Rev. Sci. Instrum. 35 (1964) 1550–1554.
[25] A. Sienkiewicz, K. Qu, Dielectric resonator-based stopped-flow electron paramagnetic resonance, Rev. Sci. Instrum. 65 (1994) 68–74.
[26] S. Pfenninger, J. Forrer, A. Schweiger, T. Weiland, Bridged loop–gap resonator: a resonant structure for pulsed ESR transparent to high-frequency radiation, Rev. Sci. Instrum. 59 (1988) 752–760.
[27] K. Qu, J.L. Vaughn, A. Sienkiewicz, C.P. Scholes, J.S. Fetrow, Kinetics and motional dynamics of spin-labeled yeast iso-1-cytochrome c: 1. Stopped-flow electron paramagnetic resonance as a probe for protein folding/unfolding of the C-terminal helix spin-labeled at cysteine 102, Biochemistry 36 (1997) 2884–2897.
[28] J.R. Anderson, R.A. Venters, M.K. Bowman, A.E. True, B.M. Hoffman, ESR and ENDOR applications of loop-gap resonators with distributed circuit coupling, J. Magn. Reson. 65 (1985) (1969) 165–168.
[29] S.M. Mattar, S.Y. Elnaggar, Analysis of two stacked cylindrical dielectric resonators in a TE102 microwave cavity for magnetic resonance spectroscopy, J. Magn. Reson. 209 (2011) 174–182 (San Diego, Calif.: 1997).
[30] S.Y. Elnaggar, R. Tervo, S.M. Mattar, Coupled modes frequencies and fields of a dielectric resonator and a cavity using coupled mode theory, J. Magn. Reson. 238 (2014) 1–7.
[31] R.R. Mett, J.W. Sidabras, I.S. Golovina, J.S. Hyde, Dielectric microwave resonators in TE011 cavities for electron paramagnetic resonance spectroscopy, Rev. Sci. Instrum. 79 (2008) 94702.
[32] J.S. Colton, L.R. Wienkes, Resonant microwave cavity for 8.5–12 GHz optically detected electron spin resonance with simultaneous nuclear magnetic resonance, Rev. Sci. Instrum. 80 (2009). 035106-035106.
[33] G. Feher, Sensitivity considerations in microwave paramagnetic resonance absorption techniques, Bell Syst. Tech. J. (1957) 449–484.
[34] J.S. Hyde, W. Froncisz, T. Oles, Multipurpose loop-gap resonator, J. Magn. Reson. 82 (1989) (1969) 223–230.
[35] G.R. Eaton, S.S. Eaton, D.P. Barr, R.T. Weber, Quantitative EPR, Springer Wien New York, Germany, 2010.
[36] G.A. Rinard, S.S. Eaton, G.R. Eaton, Poole Jr., C.P., H.A. Farach, Sensitivity in ESR measurements. Handbook Electron Spin Reson., 1999.
[37] G.A. Rinard, R.W. Quine, S.S. Eaton, G.R. Eaton, Frequency dependence of EPR sensitivity, Biol. Magn. Reson. 21 (2004) 115–154.
[38] S.Y. Elnaggar, R. Tervo, S.M. Mattar, General expressions for the Coupling Coefficient, Quality and Filling factors for a Cavity with an insert using energy coupled mode theory, J. Magn. Reson. 242 (2014) 57–66.
[39] A. Sienkiewicz, M. Jaworski, B.G. Smith, P.G. Fajer, C.P. Scholes, Dielectric resonator-based side-access probe for muscle fiber EPR study, J. Magn. Reson. 143 (2000) 144–152.
[40] A. Sienkiewicz, B. Vileno, S. Garaj, M. Jaworski, L. Forró, Dielectric resonator-based resonant structure for sensitive ESR measurements at high-hydrostatic pressures, J. Magn. Reson. 177 (2005) 261–273.
[41] D.M. Pozar, Microwave Engineering, second ed., John Wiley and Sons, Hoboken, 2005.